

# Leucaena Leucocephala Mediated Green Synthesis of Silver Nanoparticles and Their Antibacterial, Dye Degradation and Antioxidant Properties

Sandupatla Raju, Dongamanti Ashok\* and Ananda Rao Boddu

Green Medicinal Chemistry Laboratory, Department of Chemistry, Osmania University, Hyderabad-500007, Telangana, India

(\*) Corresponding author: profashokou@gmail.com  
(Received: 30 August 2021 and Accepted: 16 November 2021)

## Abstract

The current study demonstrates a green, quick and easy method for producing and characterization of silver nanoparticles from dehydrated leaf extract of *Leucaena leucocephala* (Lam-AgNPs) to evaluate its antibacterial activity against harmful bacteria, photocatalytic degradation of dyes used in textile dyeing industries and antioxidant activity to reduce oxidative stress. The UV-Visible spectra maximum absorption peak ( $\lambda_{max}$ ) of the Lam-AgNPs was noticed at 436 nm. FTIR vibrational spectra revealed the phytoconstituents that cause the reduction and stabilization of AgNPs from the plant extract. The average crystallite size was calculated to be 26 nm using the Debye-Scherrer equation with X-ray diffraction studies. The EDS spectra screening exposed a high concentration of silver with a weight % of 71.67 % and atomic % of 30.49 %. TEM studies showed the nano-sized particles that were spherical to quasi-spherical in shape and polydistributed in nature. Most particles are spread in the 15-20 nm and 30-35 nm size ranges. Lam-AgNPs had effective antibacterial action against four tested strains such as *Staphylococcus aureus*, *Bacillus subtilis*, *Pseudomonas putida* and *Klebsiella pneumoniae* by the zone of inhibition observed at 20 mm, 19 mm, 15 mm and 16 mm, respectively. The DPPH free radical scavenging assay was used to study the antioxidant activity of Lam-AgNPs and the  $IC_{50}$  value calculated was 240.70  $\mu$ g/ml. In addition, the photocatalytic activity of biogenic Lam-AgNPs for the degradation of Red m5b dye was investigated under solar light irradiation and 100% degradation was noticed after 90 minutes of reaction.

**Keywords:** Green synthesis, DPPH radical scavenging, Transmission electron microscopy, Dye degradation, Antibacterial activity.

## 1. INTRODUCTION

Because of their distinct characteristics compared to a macroscopic segment, the synthesis of novel metal nanoparticles necessitates emphasis. Metal nanoparticles are useful in various fields, including molecular imaging, drug delivery, biotechnology, optics, microelectronics, materials, medical devices for diagnosis and treatment, data storage, catalysis and energy conversion [1-8]. Silver nanoparticles (AgNPs) are non-toxic, inorganic antibacterial agents that have been utilized for centuries to destroy over 500 different types of disease-causing microorganisms [9]. Rajan et al. 2015

reported that AgNPs' non-toxic and biocompatible nature had been experimentally validated [10]. Antitumor effects [11], antibiotics [12], antibacterial effects [13, 14], wound dressings [15], nitro-aromatic compounds [16], dye degradation [17] and sensitivity to identify the prevalence of various contaminants [18] in industrial effluents are just a few of the multipurpose applications of AgNPs. This has attained the interest of many experts and encouraged them to undertake nanotechnology research. In addition, the medical domain applications such as antibacterial, antifungal, antiviral,

antioxidant, anti-inflammatory, anti-angiogenesis, antiplatelet, antitumor anticoagulant, thrombolytic, antidiabetic and anticancer activities of AgNPs have been reported earlier [19-26].

AgNPs have a large surface area to volume ratio and outstanding chemical and physical properties [27-29]. In most cases, the AgNPs generated are highly unstable, so adding a capping agent to impart stability is required. It has been widely noted that adopting a green approach using plant materials to synthesize AgNPs often results in controlled size and morphology. Furthermore, a greener method is cost-effective, environmentally benign and does not necessitate high pressure or temperature. Plant-mediated nanoparticle synthesis such as the use of medicinal plant leaves and fruit extracts has already been shown to have the potential to reduce  $\text{Ag}^+$  ions into  $\text{Ag}^0$  metallic nanoparticles [30-32]. However, there are only a few studies reported on the other parts of the plants for the same purpose [33, 34]. Numerous studies have recently demonstrated AgNPs synthesis and a variety of applications using plant extracts and microbes like *Caesalpinia bonducella* [35], *Hagenia abyssinica* [36], *Mentha longifolia* [37], *Azadirachta indica*, *Juglans regia* [38] and *Vernonia amygdalina* [39], *Acanthospermum hispidum* [40] *Mangifera indica* [41], *Saraca asoca* [42], *Ferulago macrocarpa* [43], *Aspergillus Niger* [44] and *Yeast* [45]. Due to the ever-increasing implications of incompetent chemistry practices, research into the green synthesis of AgNPs is currently receiving much attention. Meanwhile, synthesizing AgNPs with plant extracts that are widely available from natural sources is still considered to be a viable option for achieving quick and cost-effective access to such a significant material synthesis.

*Acacia gluaca* is a synonym for *Leucaena leucocephala*, and its common name is subabul [46]. The plant is a medium-sized, fast-growing tree that belongs to the *Fabaceae* family. *Leucaena*

*leucocephala* has outstanding medicinal properties such as stomach ache, contraception and abortifacient. The sulphated glycosylated polysaccharides from seeds were found to have significant cancer chemo-preventive and anti-proliferative properties [47]. The seed gum is utilized as a binder in tablet formulations [48, 49]. These plant extracts have antidiabetic, antibacterial and anti-helminthic properties [50, 51]. The leather and cotton industries can benefit from the colors derived from this plant [52]. Because of its many applications, the plant is referred as a miracle tree [53].

Hence, the current study adopted a green approach to synthesizing AgNPs using dehydrated leaf extracts of *Leucaena leucocephala*, a medicinally important plant. The leaf extract is employed as both reducing as well as stabilizing agent. The principal pollutants used in the textile industry are dyes, which are later combined with freshwater and deposited somewhere on the earth, resulting in water and earth pollution. So treating this water was an important environmental task. Finding novel antimicrobial agents to treat most diseases is also a critical challenge. Oxidative stress caused by a person's lifestyle can also contribute to the development of cancer and other diseases. So, oxidative stress reduction also has significance. Therefore, the purpose of this study is to synthesize AgNPs from leaf extracts of *Leucaena leucocephala* (Lam-AgNPs), characterize the synthesized Lam-AgNPs and evaluate their photocatalytic degradation of textile dye, antioxidant and antibacterial activities.

## 2. EXPERIMENTAL

### 2.1. Chemicals

Fresh *Leucaena leucocephala* leaves were collected from the Osmania University campus, Hyderabad, Telangana, India. AR grade silver nitrate was purchased from SD Fine Chemicals, Mumbai, India. From Himedia Laboratories, Mumbai, India, the

chemicals used for antibacterial investigation were obtained. The glassware used in this study was acid-washed, followed by a thorough rinse with distilled water. The dye was obtained from a small dyeing industry in Rajanna Sircilla District, Telangana, India. The bacterial test strains were procured from IMTECH, Chandigarh, India.

## 2.2. Preparation of Plant Extract

The leaf extract was prepared by a method similar to that used by Selvaraj et al. 2015 [54]. Fresh and disease-free leaves from the plant *Leucaena leucocephala* shown in Figure 1a were collected and then thoroughly washed under running tap water to remove the adhered dust particles on the surface, followed by rinsing with distilled water. The washed leaves were then dried under shade at room temperature for 10 days on a filter paper. The dried leaves were then crushed into small pieces and ground to a fine powder using mortar and pestle. The aqueous leaves extract of *Leucaena leucocephala* was prepared by mixing 5gm of leaf powder with 1000ml of distilled water and then incubated overnight at room temperature to extract phytochemicals. The clear solution with phytochemicals was collected by filtering through Whatman No.1 filter paper, as shown in Figure 1b. The leaf extract filtrate thus obtained was collected in a screw-capped bottle and stored in a refrigerator, which was later used for the green synthesis of Lam-AgNPs.

## 2.3. Preparation of Silver Nitrate Solution

A fresh stock solution of 1mM  $\text{AgNO}_3$  was prepared by dissolving the required solid  $\text{AgNO}_3$  in double-distilled water as shown in Figure 1c and storing it in a brown-colored bottle to prevent photo-degradation of silver.

## 2.4. Synthesis of Lam-AgNPs

500ml of leaf extract was added to 500ml of silver nitrate solution dropwise at room temperature while stirring to synthesize Lam-AgNPs. The color of the solution changes from pale yellow to dark brown after 10 minutes of reaction. The brown color in Figure 1d indicates the formation of Lam-AgNPs. The characteristic red-brown color of AgNPs is caused by surface plasmon resonance (SPR). To complete the reduction, the reaction is allowed to run for 3 hours. The colloidal Lam-AgNPs solution was centrifuged for 15 minutes at 10000rpm, and the concentrated colloidal Lam-AgNPs was collected. To eliminate the extra-biological materials, it was washed twice by repeating the centrifugation with distilled water and dried for one day in a hot air oven at 60°C. The dried powder was scraped up and ground with a pestle to produce a fine Lam-AgNPs powder that can be used in further research.

## 2.5. Characterization of Lam-AgNPs

After the reaction, colloidal nanoparticle suspension is combined with distilled water and UV-Vis spectroscopy with wavelength range of 200-800 nm is employed. The formation of stable Lam-AgNPs by reducing  $\text{Ag}^+$  ions was monitored by UV-Vis spectrum analysis, carried out with the Shimadzu UV 2600 UV-Vis Spectrophotometer. The KBr pellet was made from 1mg of synthesized Lam-AgNPs compressed with a small amount of potassium bromide and used for Fourier transform infrared spectroscopy (FTIR) examination. The IR Affinity-1, Shimadzu Model was used to record the FTIR of synthesized Lam-AgNPs with a wavenumber range of 4500-500  $\text{cm}^{-1}$ . The X-ray diffraction analysis (XRD) of Lam-AgNPs is performed using Philips Xpert Pro equipment with a  $\text{CuK}\alpha$  X-ray source, 40kV, 30mA generator settings and a scanning rate of 2  $\text{min}^{-1}$  in  $\theta=2\theta$  configuration. Model ZEISS Special edition 18 instrument was used to capture

scanning electron microscopy (SEM) pictures of synthesized Lam-AgNPs. The SEM images are obtained by developing a thin film of the colloidal sample by dropping a small amount of sample on a carbon-coated copper grid and allowing it to dry at room temperature. The elements that correspond to the peaks in the energy distribution are automatically identified using SEM coupled energy-dispersive x-ray spectroscopy (EDS) technology. A small amount of metallic nanopowder was

disseminated in 1ml of distilled water and then sonicated for 30 minutes in an ultrasonic water bath to produce transmission electron microscopy (TEM) pictures.

A drop of the sample is deposited on a carbon-coated copper grid placed on parafilm and the excess is drained with filter paper and the sample is allowed to dry for 5-10 minutes. Later, using the Hitachi H-7500 model, the TEM images at various magnifications were obtained.



**Figure 1.** (a) *Leucaena leucocephala* plant (b) aqueous leaves extract of *Leucaena leucocephala* (c) Silver Nitrate solution (d) green synthesized Silver nanoparticles.

## 2.6. Antibacterial Activity

The well-diffusion method [55] was used to investigate the antibacterial activity of produced Lam-AgNPs. Antibacterial experiments were performed on four microorganisms, including *Klebsiella pneumoniae*, *Bacillus subtilis*, *Staphylococcus aureus* and *Pseudomonas putida* using fresh cultures and sterilized labware. The bacteria were cultured on nutrient agar medium prepared by dissolving 2.8gm of nutrient agar in 100ml of distilled water and autoclaving. The sterilized media was poured into the petriplates and allowed to solidify. After that, each plate was inoculated with 50 $\mu$ l of specific bacteria. A sterile borer was used to make wells in various locations on the petriplates. Then appropriate samples were added and incubated for 12 hours at 37°C to study the zone of inhibition.

## 2.7. DPPH Free Radical Scavenging Assay

The antioxidant activity of Lam-AgNPs was tested using the DPPH (2, 2-diphenyl-1-picrylhydrazyl) free radical scavenging assay. Serial dilutions from a stock solution of 1mg/1ml in distilled water produced five different concentrations of synthesized Lam-AgNPs as 25, 50, 100, 200 and 400  $\mu$ g/ml. The positive control used is ascorbic acid (1mg/1ml). In test tubes, 1ml of each concentration was mixed with 3ml of methanol solution containing 0.1mM DPPH radicals. The sample tubes are vigorously shaken and kept at room temperature for 30 minutes. The absorbance of DPPH was measured using UV-Vis spectroscopy at 517 nm. As a blank solution, methanol is employed. The control sample was a DPPH methanolic solution devoid of Lam-AgNPs. The results are represented graphically using MS Excel as IC<sub>50</sub> values.

A linear regression plot was drawn between Lam-AgNPs concentration and DPPH inhibition%. The following equation was used to compute the inhibition% for the radical scavenging experiments.

$$AA\% = [(A_{\text{Control}} - A_{\text{Sample}}) / A_{\text{Control}}] \times 100 \quad (1)$$

Here, AA% absorption of antioxidant

$A_{\text{Control}}$ -absorption of the ascorbic acid

$A_{\text{Sample}}$ -absorption after addition of Lam-AgNPs for each concentration.

## 2.8. Photocatalytic Activity

The photocatalytic activity of green synthesized Lam-AgNPs was carried out to study the degradation of reactive textile dye Red m5b while exposed to sunlight. The method for photocatalytic activity was similar to Venkatesham et al. 2014 and Jegadeeswaran et al. 2012 [56, 57]. 1mg of dye was dissolved in 100ml distilled water and divided into two equal parts in beakers. One beaker was marked as a control and the other as a sample. 10mg of produced silver nanoparticles were directly added to the sample beaker and constantly stirred under the sunlight. To compare the degradation% of the Red m5b dye, a control beaker was kept under similar conditions. At every 15 minute time interval, 4ml of the colloidal dye mixture solution was taken and centrifuged at 5000rpm for 10 minutes to remove Lam-AgNPs from the colloidal dye solution. The dye degradation percentage in the collected supernatant was examined using UV-Vis spectroscopy.

## 3. RESULTS AND DISCUSSION

### 3.1. UV-Vis Spectroscopy

The UV-Vis spectrum [58] of the colloidal solution was used to determine the bioreduction of  $\text{Ag}^+$  ions into phytochemical-stabilized  $\text{Ag}^0$  by the leaf extract of *Leucaena leucocephala* [59]. UV-Vis spectroscopy is the most widely used technique for the characterization of nanoparticles. The initial color of the reaction mixture after adding the leaves extract to the aqueous  $\text{AgNO}_3$  solution was

colorless. The color of the colloidal solution changed from pale yellow to dark brown after the reaction. Due to the stimulation of surface plasmon resonance (SPR), AgNPs exhibit deep brown color when the reaction proceeds. Metallic silver nanoparticles exhibit the SPR is a characteristic optical phenomenon induced by the mutual vibration of electrons when striking the UV-Visible light. Figure 2a shows the UV-Vis spectra of *Leucaena leucocephala* leaf extract and synthesized colloidal Lam-AgNPs. The maximum absorption peak ( $\lambda_{\text{max}}$ ) of the Lam-AgNPs was observed at 436 nm. Similar UV-visible spectra results were observed in *Solanum torvum* mediated AgNPs ( $\lambda_{\text{max}}$  at 434nm) reported by Govindaraju et al. 2010 [60] and *Gliricidia sepium* mediated AgNPs ( $\lambda_{\text{max}}$  at 440nm) reported by Raut et al. 2009 [61]. The absorbance between 400-450nm in UV-Vis spectroscopy is the characteristic peak for silver nanoparticles and the peak designates the development of colloidal silver nanoparticles [62, 63]. Furthermore, a flat curve indicates that the formed colloidal Lam-AgNPs contain polydistributed nanoparticles.

### 3.2. FTIR Analysis

The FTIR study revealed shifts and variations in the regions of the peaks could affect the results. The correlation of the vibrational bands with the chemical compounds employed in the sample is interpreted with the FTIR spectra. It was proved by FTIR spectroscopy that the phytochemical biomolecules present in extracts of *Leucaena leucocephala* leaves are responsible for the reduction and stabilization processes of nanoparticles. Flavonoids, terpenoids, proteins and polyphenols can be found in abundance in the dried leaves of the *Leucaena leucocephala* plant. The primary FTIR vibrational peaks shown in Figure 2b of Lam-AgNPs were observed at  $1534\text{cm}^{-1}$ ,  $1379\text{cm}^{-1}$ ,  $1197\text{cm}^{-1}$ ,  $1056\text{cm}^{-1}$  and  $704\text{cm}^{-1}$ . The N-H bending vibrations in the amide II links of proteins [64, 65] are represented

by the band at  $1534\text{cm}^{-1}$ , whereas C-H rock alkenes are represented by the band at  $1379\text{cm}^{-1}$ . The C-N stretching vibrations of aliphatic amines or -OH bending vibrations of polyphenols induce the strong bands at  $1197\text{cm}^{-1}$  and  $1056\text{cm}^{-1}$ . The abundant involvement of polyphenols [66, 67] as capping agents on the exterior of nanoparticles could explain the rise in the intensity of the band. The peaks at  $704\text{cm}^{-1}$  produced by CH-out plane bending vibrations caused by substituted ethylene systems -CH=CH. The FTIR spectral data of Lam-AgNPs clearly shows that proteins and polyphenols are involved in the Lam-AgNPs reduction process. They serve as capping agents for the AgNPs particles and stabilize them. The FTIR vibrational spectra of Lam-AgNPs reported by Gotekar et al. 2018 [68] using the same plant *Leucaena leucocephala* concludes the phenolic compounds involvement in the stabilization. But a vibrational band at  $3630\text{cm}^{-1}$  was not observed in our FTIR spectra, which may be due to differences in the plant extract preparation and AgNPs synthesis procedure.

### 3.3. X-ray Diffraction

X-ray diffraction study of green synthesized Lam-AgNPs was conducted to confirm their crystalline structure. Lam-AgNPs have four unique  $2\theta$  diffraction peaks found at  $37.72^\circ$ ,  $43.88^\circ$ ,  $64.13^\circ$  and  $77.13^\circ$ . Figure 2c illustrates these diffraction peaks are understood to be (1 1 1), (2 0 0), (2 2 0) and (3 1 1) lattice planes respectively. These XRD values indicate the face-centric cubic crystalline (FCC) structure of Lam-AgNPs [69] (JCPDS file:65-2871). The other unassigned peaks were arises due to the cubic face of AgCl nanoparticles those corresponding to the (1 1 1), (2 0 0), (2 2 0), (3 1 1) and (2 2 2) planes (JCPDS file: 31-1238). The Debye-Scherer formula was used to calculate the crystalline size of the produced Lam-AgNPs. The crystallite size ranges from 18 to 33 nm, with an average size of 26 nm.

$$D = \frac{K\lambda}{\beta_{0.5} \cos \theta} \quad (2)$$

Where  $D$  is the crystalline size of Lam-AgNPs,  $\lambda$  is the wavelength of the X-ray source (0.1541 nm),  $\beta$  is the full width at half maximum (FWHM) of the diffraction peak,  $K$  is the Scherrer constant with a value of 0.9-1 and  $\theta$  is the Bragg's angle in radian. The principal peaks identified in XRD data and their lattice parameter values were calculated. The average was determined to be 4.1, which was very close to the standard silver nanoparticle lattice parameter value of 4.085. The current XRD results suggest the synthesized nanoparticles are a mixture of Ag and AgCl NPs. The results were confirmed by EDS analysis. Similar XRD patterns were reported for AgNPs preparations using *Megaphrynium macrostachyum* leaf extract by Francois et al. 2016 [70], *Ipomoea batata* leaf extract by Awwad et al. 2013 [71] and *Albizia julibrissim* flower extract by Awwad et al. 2015 [72].

**Table 1.** Lattice parameter values for the peaks at  $2\theta$  Positions.

Position [ $2\theta$ ]	FWH M [ $2\theta$ ]	$d$ -spacin g [ $\text{\AA}$ ]	$hkl$	Lattice parameter
37.72	0.3149	2.3846	111	4.12
43.88	0.3149	2.0632	200	4.12
64.13	0.4723	1.4520	220	4.09
77.13	0.3840	1.2356	311	4.07

### 3.4. SEM-EDS

SEM was used to examine the surface morphology of the Lam-AgNPs. As shown in Figure 3a, Lam-AgNPs are mainly quasi-spherical shaped and nano-sized particles with smooth surfaces. The elemental composition profile of the produced Lam-AgNPs was clearly visible in the dispersive energy spectrum in Figure 3b, indicating the presence of silver as an ingredient element. Due to surface plasmon resonance [71], metallic silver nanoparticles often exhibit an optical absorption peak at  $\sim 3$  keV.

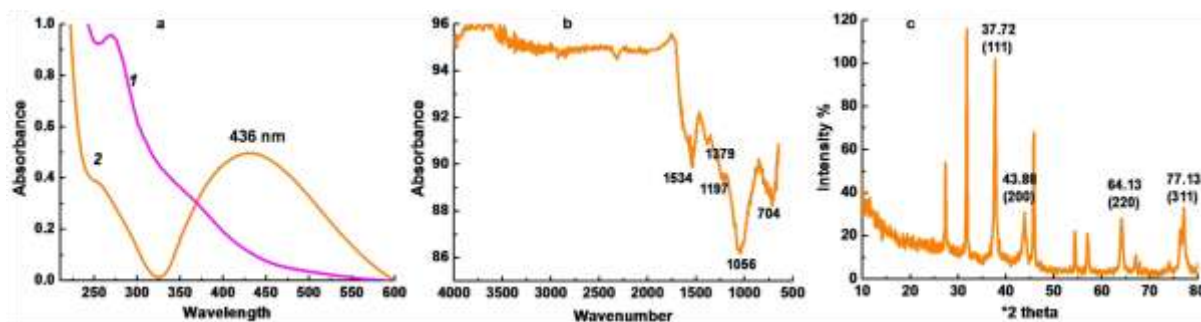


**Figure 2.** (a) UV-Vis spectroscopy of (1) *Leucaena leucocephala* leaves extract (2) Lam-AgNPs (b) FTIR Spectra of Lam-AgNPs (c) XRD pattern of Lam-AgNPs.

Other peaks (C, O) were most likely connected to the phytochemical components in the leaf extract. The high content of the Cl element was due to the mixture of AgCl and AgNPs in the

synthesized material. The table within the image of the EDS spectra revealed a high concentration of silver with 71.67% as weight % and 30.49% as atomic%.

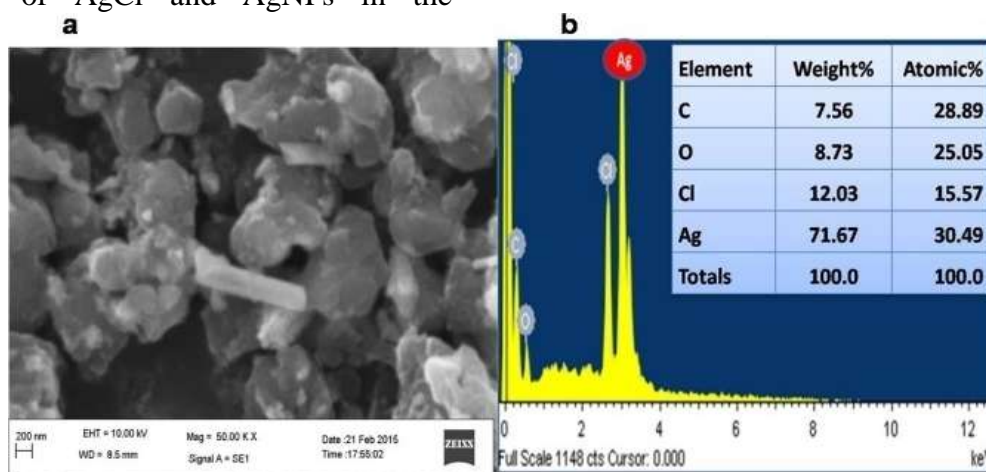


**Figure 3.** (a) SEM image of Lam-AgNPs (b) Energy dispersive X-ray spectrum (EDS) and elemental analysis of Lam-AgNPs.

### 3.5. TEM Analysis

The size, shape and morphology of the particles were studied using TEM microscopic instrument analysis. The TEM images of the produced Lam-AgNPs depicted in Figure 4a showed clear pictures of nano-sized particles that were polydistributed and monoclinic in nature. No aggregation was observed in the TEM images of Lam-AgNPs and they have an average size of 31 nm, which was greater than the size of Lam-AgNPs identified with XRD data. Biomolecules from the *Leucaena leucocephala* leaf extract such as phytochemicals were found to be encapsulating the particles. The size distribution of silver nanoparticles is

depicted in the histogram of synthesized Lam-AgNPs shown in Figure 4b.

Most particles are spread in the 15-20nm and 30-35nm diameter range. Similar TEM results were reported by Azarbani and Shiravand 2020 and demonstrated that the AgNPs were spherical with diameters ranging from 14-25nm [43]. Shahin peral et al. 2021 synthesized AgNPs using *Rosa damascena* were nearly spherical to quasi-spherical shape and ranged from 8.6-49.7nm [73].

### 3.6. Antibacterial Activity

Silver's well-known inhibitory action has been known for several years and used in various medicinal applications [74].

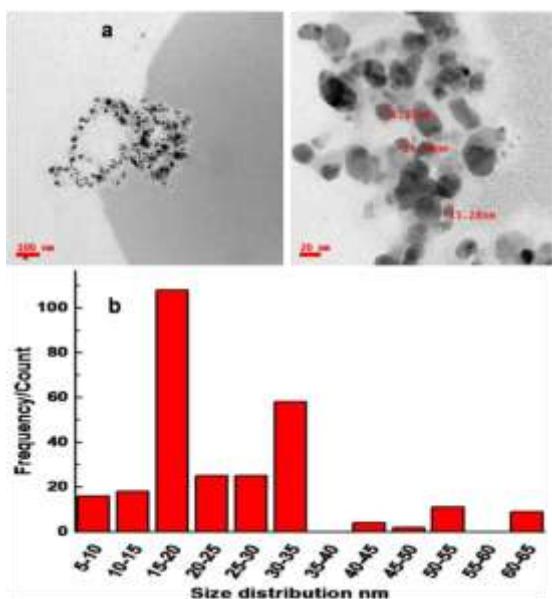


**Figure 4.** (a) TEM images of Lam-AgNPs nano-sized particles (b) Histogram of the size distribution of Lam-AgNPs.

The well-diffusion method was used to test the antibacterial activity. Lam-AgNPs had effective antibacterial action against four tested strains such as *Staphylococcus aureus*, *Bacillus subtilis*, *Pseudomonas putida* and *Klebsiella pneumoniae* and zones of inhibition were observed at 20mm, 19mm, 15mm and 16mm respectively. AgNPs of 20nm size with antibacterial action against numerous gram-negative and gram-positive microbes were synthesized using dried leaves of *Pongamia pinnata* [75] and less zone of inhibition was observed than our current report. However, Suresh Gotekar et al. 2018 [68] reported a high zone of inhibition in the case of AgNPs synthesized using the same plant *Leucaena leucocephala* when they used the highest concentration of 500 µg/ml against various pathogens. The highest activity was observed in the case of both gram-positive bacteria. The fundamental difference between gram-positive and gram-negative bacteria is the structure of their cell walls, which affects their antibiotic susceptibility. A gram-positive organism has a thick layer of peptidoglycan rather than an outer (LPS) membrane. This makes it easier for cell-wall active AgNPs

to get to their target. The same statement was supported by the previous report of Muthuvel et al. 2020 [76]. The zone of inhibition was exhibited as the bar diagram shown in Figure 5.

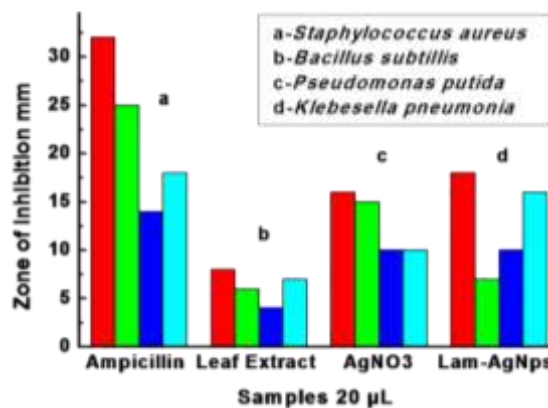


**Figure 5.** Bar diagram of Lam-AgNPs indicating the zone of inhibition for four tested bacteria.

The synthesized Lam-AgNPs exert good antibacterial efficacy against all four microorganisms tested compared to the leaf extract and AgNO<sub>3</sub>. In the case of *Pseudomonas putida*, high activity was observed more than the controlled drug. The maximum conductivity of cells treated with Lam-AgNPs caused the disruption of cell walls and released biological components existing inside the cells. The same was reported in the antibacterial action of nanoparticles on microbes by Abebe et al. 2020 [77]. The present study with advanced clinical experiments could set a new standard for developing novel antibacterial medications.

### 3.7. DPPH Free Radical Scavenging Assay

DPPH is an organic nitrogen-centered radical and frequently employed to diminish the antioxidant's potency. When DPPH is dissolved in methanol, it produces a purple color and is reduced in the presence of antioxidant molecules resulting in a colorless methanol solution. This approach relies on a hydrogen-donating antioxidant to produce DPPHH, a non-radical version of DPPH.

Synthesized Lam-AgNPs have free radical scavenging activity that is dose-dependent. Table 2 shows the results of the DPPH radical scavenging assay, including %inhibition and IC<sub>50</sub>(µg/ml) values.

**Table 2.** DPPH radical scavenging assay with % of inhibition and IC<sub>50</sub>(µg/ml).

Lam-AgNPs µg/ml	Abs.	% of inhibition	IC <sub>50</sub> µg/ml
25	1.12	15.15	240.70
50	0.992	24.84	
100	0.898	31.96	
200	0.620	53.03	
400	0.428	67.57	
Control	1.32	00	
Ascorbic acid	0.058	95.60	

The lowest scavenging activity observed was 15.15% and the highest was found to be 67.57% of inhibition. The ascorbic acid employed as a positive control in this investigation inhibited DPPH by 95.60%. The IC<sub>50</sub> value calculated through the linear regression graph is 240.70µg/ml. A similar % DPPH of inhibition results were noticed by Achytha kumar Biswal et al. 2020 [78], eventhough they used high concentrations of AgNPs. They reported that the lowest concentration of the AgNPs (5mg/ml) was found to be 19.34±0.15 which increased to 65.45±0.10 when the concentration was increased to 20mg/ml. Nsimba et al. 2008 [79] found that *Chenopodium quinoa* and *Chenopodium album* mediated AgNPs exhibited a marginal increase in antioxidant activity of plant-AgNPs over plant extract and suggested that the plant extract is responsible for the majority of the antioxidant activity. The findings show that the green Lam-AgNPs nanoparticles serve as free radical scavengers.

### 3.8. Photocatalytic Activity

Under sunlight irradiation, the photocatalytic activity of green synthesized Lam-AgNPs was tested using Red m5b

dye, commonly used in the textile sector. The dye degradation was visibly observed as the color of the solution changed from pink to colorless over time. Red m5b has two primary absorption peaks ( $\lambda_{max}$ ) at 510nm and 540nm. The degradation of the dye in the presence of biogenic Lam-AgNPs was monitored by UV-Vis spectra that showed a drop in peak intensity after 90 minutes of exposure to sunlight, as shown in Figure 6a. The continuous decrease of peak intensity (hypochromic shift) implies that the dye solution gradually degrades. The color change signifies the degradation of organic dye under solar light irradiation and the reduction of the dye is a thermodynamically favourable process. The findings show that removing the chromophore group from dye molecules is due to significant structural changes caused by Lam-AgNPs. When exposed to sunlight, the control showed no change in coloration. For each time interval, the dye degradation percent is determined using the below formula.

Solar light was found to be more effective than other irradiation techniques. The catalytic degradation process begins when sunlight photons strike colloidal AgNPs. The earlier reports of degradation mechanisms involved the excitation of conduction electrons of metallic Ag and dyes. The electrons on the particle surface are activated by photons that strike the nanoparticles in the colloidal mixture when exposed to sunlight. The excited electrons from the particle surface interact with the dissolved oxygen molecules in the reaction medium and convert them to oxygen anion radicals. These radicals break down the organic dye into smaller organic molecules and cause degradation quickly. Hence, the utilization of green synthesized Lam-AgNPs in the degradation of organic dyes in the presence of solar light proved that they are very stable photocatalysts [80].

Dye degradation (%) =  $[(C_0 - C_t) / C_0] \times 100$  where  $C_t$  is the concentration of the dye solution after t minutes of exposure to

sunlight irradiation and  $C_0$  is the initial concentration of the Red m5b dye. The control sample exhibited an initial optical density (OD) at 0.129. As shown in Figure 6b, the percentage of textile dye

degradation after 15 minutes of reaction was 55.81% and increased to 100% after 90 minutes of reaction exposure. The results imply the gradual degradation of dye at various time intervals.

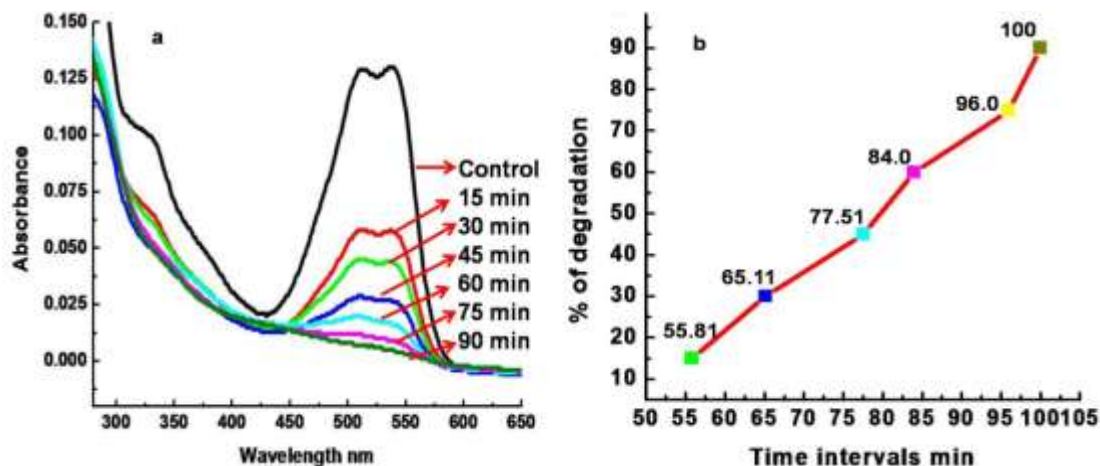


**Figure 6.** (a) UV-Vis Spectroscopy of degradation of textile dye Red m5b (b) The degradation % of textile dye for every 15 mins of the time interval.

#### 4. CONCLUSION

In conclusion, the fabrication of nanoparticles has increased interest due to the rising demand to bring about safe and low-cost methods for nanomaterial synthesis. The green synthesis of silver nanoparticles has emerged as a simpler and better alternative to physical and chemical procedures since it is a quick, clean and environmentally friendly approach that does not require expensive instruments. So, developing a natural and phytomediated experimental approach for nanoparticle manufacturing is becoming a significant nanotechnology derivative. *Leucaena leucocephala* leaf extract is capable of reducing the ionic Ag to stable Lam-AgNPs from silver nitrate solution as a precursor. Spectroscopic and microscopic techniques such as UV-Vis spectroscopy, FTIR, XRD, SEM-EDS and TEM were employed to characterize the green synthesized Lam-AgNPs. The green synthesized Lam-AgNPs were found to be spherical to quasi-spherical in shape, with an average diameter of 31 nm. According to the findings, Lam-AgNPs synthesized from *Leucaena leucocephala* leaf extract

provide efficient bioactive components for bacterial growth suppression. The antioxidant activity proved that Lam-AgNPs are important factors in reducing oxidative stress. The photocatalytic investigation found that these biogenic silver nanoparticles effectively degrade Red m5b when exposed to sunlight. So, these Lam-AgNPs could be employed to treat polluted water as an environmental concern. The current method could be useful in developing other metal nanoparticle-based stable systems.

#### ACKNOWLEDGEMENT

The authors are grateful to the Forensic Science Unit of the Department of Chemistry for providing the research facilities. The authors are thankful to the University Grants Commission, New Delhi, India for awarding Sandupatla Raju with a Senior Research Fellowship and D. Ashok with a BSR Fellowship.

#### CONFLICT OF INTEREST

The authors declare that they have no conflict of interest.

## REFERENCES

1. Meng, H., Liang, M., Xia, T., Li, Z., Ji, Z., Zink, J. I., Nel, A. E., “Engineered design of mesoporous silica nanoparticles to deliver doxorubicin and P-glycoprotein siRNA to overcome drug resistance in a cancer cell line”, *ACS Nano*, 4(8) (2010) 4539–4550.
2. Yang, F., Jin, C., Subedi, S., Lee, C. L., Wang, Q., Jiang, Y., Li, J., Di, Y., Fu, D., “Emerging inorganic nanomaterials for pancreatic cancer diagnosis and treatment”, *Cancer. Treat. Rev.*, 38(6) (2012) 566–579.
3. Mout, R., Moyano, D. F., Rana, S., Rotello, V. M., “Surface functionalization of nanoparticles for nanomedicine”, *Chem. Soc. Rev.*, 41(7) (2012) 2539–2544.
4. Mathew, T. V., Kuriakose, S., “Studies on the antimicrobial properties of colloidal silver nanoparticles stabilized by bovine serum albumin”, *Colloids. Surf. B Biointerfaces*, 101 (2013) 14–18.
5. Bindhu, M. R., Umadevi, M., “Synthesis of monodispersed silver nanoparticles using Hibiscus cannabinus leaf extract and its antimicrobial activity”, *Spectrochim. Acta. A*, 101 (2013) 184–190.
6. Tamuly, C., Hazarika, M., Borah, S. C., Das, M. R., Boruah, M. P., “In situ biosynthesis of Ag, Au and bimetallic nanoparticles using Piper pedicellatum C.DC: green chemistry approach”, *Colloids Surf. B. Biointerfaces*, 102 (2013) 627–634.
7. Rafiuddin, Z. Z., “Silver nanoparticles formation using tyrosine in presence acetyltrimethylammonium bromide”, *Colloids Surf. B. Biointerfaces*, 89 (2012) 211–215.
8. Abebe, B., Ananda Murthy, H. C., Dessie, Y., “Synthesis and Characterization of Ti–Fe Oxide Nanomaterials: Adsorption–Degradation of Methyl Orange Dye”, *Arabian Journal for Science and Engineering*, 45(6) (2020) 4609–4620.
9. Cheng, K., Hung, Y., Chen, C., Liu, C., Young, J., “Green synthesis of chondroitin sulfate-capped silver nanoparticles: characterization and surface modification”, *Carbohydr. Polym.* 110 (2014) 195–202.
10. Rajan, R., Chandran, K., Harper, S. L., Yun, S. I., Kalaichelvan, P. T., “Plant extract synthesized silver nanoparticles: An ongoing source of novel biocompatible materials”, *Industrial Crops and Products*, 70 (2015) 356–373.
11. Jeyaraj, M., Sathishkumar, G., Sivanandhan, G., Mubarak Alid, D., Rajesh, M., Arun, R., Kapildev, G., Manickavasagam, M., Thajuddin, N., Premkumar, K., Ganapathi, A., “Biogenic silver nanoparticles for cancer treatment: an experimental report”, *Colloids Surf. B. Biointerfaces*, 106 (2013) 86–92.
12. Singh, K. P., Singh, A. K., Gupta, S., Rai, P., “Modeling and optimization of reductive degradation of chloramphenicol in aqueous solution by zero-valent bimetallic nanoparticles”, *Environ. Sci. Pollut. Res.*, 19(6) (2012) 2063–2078.
13. Kumar, P. P. N. V., Pammi, S. V. N., Kollu, P., Satyanarayana, K. V. V., Shameem, U., “Green synthesis and characterization of silver nanoparticles using Boerhaavia diffusa plant extract and their antibacterial activity”, *Ind. Crops Prod.*, 52 (2014) 562–566.
14. Khan, M., Khan, S.T., Khan, M., Adil, S. F., Musarrat, J., Al-Khedhairi, A. A., Alkhatlan, H. Z., “Antibacterial properties of silver nanoparticles synthesized using Pulicaria glutinosa plant extract as a green bioreductant”, *Int. J. Nanomed.*, 9 (2014) 3551–3565.
15. Rakgoshi, L., Blessing A. A., Shesan John O., Emanuel R., Youmbi T. F., Derek T. N., Suprakas S. R., “Gum Acacia/Carbopol-Based Biocomposites Loaded with Silver Nanoparticles as Potential Wound Dressings”, *Int. J. Nanosci. Nanotechnol.*, 16(4) (2020) 219–231.
16. Narayanan, K. B., Sakthivel, N., “Heterogeneous catalytic reduction of anthropogenic pollutant, 4-nitrophenol by silver-bionanocomposite using *Cylindrocylindrum floridanum*. Bioresour”, *Technol.*, 102 (2011) 10737–10740.
17. Kumar, P., Govindarajua, M., Senthamilselvi, S., Premkumar, K., “Photocatalytic degradation of methyl orange dye using silver (Ag) nanoparticles synthesised from *Ulva lactuca*”, *Colloids Surf. B. Biointerfaces*, 103 (2013) 658–661.
18. Balavigneswaran, C. K., Sujin Jeba Kumar, T., Moses Packiaraj, R., Prakash, S., “Rapid detection of Cr(VI) by AgNPs probe produced by *Anacardium occidentale* fresh leaf extracts”, *Appl. Nanosci.*, 4(3) (2014) 367–378.
19. Elegbede, J., Lateef, A., “Nanotechnology in the built environment for sustainable development”, *IOP Conference Series Materials Science and Engineering*, 805(1) (2020) 012044.
20. Agbaje, L., Elegbede, J. A., Akinola, P. O., Ajayi, V. A., “Biomedical applications of green synthesized-metallic nanoparticles: A review”, *Pan African Journal of Life Sciences*, 3(1) (2019) 157–182.
21. Badmus, J. A., Oyemomi, S. A., Adedosu, O. T., Yekeen, T. A., Azeez, M. A., Adebayo, E. A., Lateef, A., Badeggi, U. M., Botha, S., Hussein, A. A., Marnewick, J. L., “Photo-assisted bio-fabrication of silver nanoparticles using *Annona muricata* leaf extract: Exploring the antioxidant, antidiabetic, antimicrobial, and cytotoxic activities”, *Heliyon*, 6(11) (2020) e05413.
22. Aina, D. A., Owolo, O., Lateef, A., Aina, F. O., Hakeem, A. S., Adeoye-Isijola, M., Okon, V., Asafa, T. B., Elegbede, J. A., Olukanni, O. D., Adediji, I., “Biomedical Applications of *Chasmanthera dependens* stem

- extract mediated silver nanoparticles as Antimicrobial, Antioxidant, Anticoagulant, thrombolytic and Larvicidal agents, *Karbala International Journal of Modern Science*, 5(2) (2019) 71–80.
23. Oladipo, I. C., Lateef, A., Azeez, M. A., Asafa, T. B., Yekeen, T. A., Ogunsona, S. B., Irshad, H. M., Abbas, S. H., “Antidiabetic properties of phytosynthesized gold nanoparticles (Aunps) from *Datura stramonium* seed, *IOP Conference Series Materials Science and Engineering*, 805 (2020) 012035.
  24. Lateef, A., Ojo, S. A., Elegbede, J. A., Akinola, P. O., Akanni, E. O., “Nanomaterial applications of nanoparticles for blood coagulation disorders”, *Environmental Nanotechnology*, Springer International Publishing, 1 (2018) 243–277.
  25. Gomathi, A. C., Xavier Rajarathinam, S. R., Mohammed Sadiq, A., Rajeshkumar, S., “Anticancer activity of silver nanoparticles synthesized using aqueous fruit shell extract of *Tamarindus indica* on MCF-7 human breast cancer cell line”, *Journal of Drug Delivery Science and Technology*, 55 (2020) 101376.
  26. Tessy, J., Kokila, A., Parmar, S., Shailesh, C., Kotval, J., Jayesh, J., “Synthesis, Characterization, Antibacterial and Anticancer Properties of Silver Nanoparticles Synthesized from *Carica Papaya* Peel Extract”, *Int. J. Nanosci. Nanotechnol.*, 17(1) (2021) 23-32.
  27. Kurek, A., Grudniak, A. M., Kraczkiewicz-Dowjat, A., Wolska, K. I., “New antibacterial therapeutics and strategies”, *Pol. J. Microbiol.*, 60(1) (2011) 3-12.
  28. Mathew, T. V., Kuriakose, S., “Studies on the antimicrobial properties of colloidal silver nanoparticles stabilized by bovine serum albumin”, *Colloids Surf. B. Biointerfaces*, 101 (2013)14-18.
  29. Vijayaraghavan, K., Nalini, S. P. K., Prakash, N. U., Madhankumar, D., “One step green synthesis of silver nano/microparticles using extracts of *Trachyspermum ammi* and *Papaver somniferum*”, *Colloids Surf. B. Biointerfaces*, 94 (2012) 114–117.
  30. Daniel, S. C. G. K., Kumar, R., Sathish, V., Sivakumar, M., Sunitha, S., Sironmani, T. A., “Green Synthesis (*Ocimum tenuiflorum*) of Silver Nanoparticles and Toxicity Studies in Zebra Fish (*Danio rerio*)”, *Int. J. Nanosci. Nanotechnol.*, 2(2) (2011) 103–117.
  31. Sulochana, S., Krishnamoorthy, P., Sivaranjani, K., “Synthesis of Silver Nanoparticles using Leaf Extract of *Andrographis paniculata*”, *J. Pharmacol. Toxicol.*, 7(5) (2012) 251–258.
  32. Ghaffari-Moghaddam, M., Hadi-Dabanlou, R., “Plant mediated green synthesis and antibacterial activity of silver nanoparticles using *Crataegus douglasii* fruit extract” *J. Ind. Eng. Chem.*, 20 (2014) 739–744.
  33. Roopan, S. M., Rohit, G. M., Madhumitha, G., Rahuman, A. A., Kamaraj, C., Bharathi, A., Surendra, T., “Low-cost and eco-friendly phyto-synthesis of silver nanoparticles using *Cocos nucifera* coir extract and its larvicidal activity”, *Ind. Crop Prod.*, 43 (2013) 631–635.
  34. Saxena, A., Tripathi, R. M., Singh, R. P., “Biological synthesis of silver nanoparticles by using onion (*Allium cepa*) extract and their antibacterial activity”, *Dig. J. Nanomater. Bios.*, 5(2) (2010) 427–432.
  35. Sukumar, S., Rudrasenan, A., Padmanabhan Nambiar, D., “Green-synthesized rice-shaped copper oxide nanoparticles using *Caesalpinia bonducella* seed extract and their applications”, *ACS Omega*, 5(2) (2020) 1040–1051.
  36. Murthy, H. C. A., Desalegn, T., Kassa, M., Abebe, B., Assefa, T., “Synthesis of green copper nanoparticles using medicinal plant *Hagenia abyssinica* (Brace) jf. Gmel. leaf extract: Antimicrobial properties”, *Journal of Nanomaterials*, (2020) 1–12.
  37. Javed, B., Nadeem, A., Mashwani, Z. R., “Phytosynthesis of Ag nanoparticles from *Mentha longifolia*: Their structural evaluation and therapeutic potential against HCT116 colon cancer, Leishmanial and bacterial cells”, *Applied Nanoscience*, 10(9) (2020) 3503–3515.
  38. Paseban, N., Ghadam, P., Purohosseini, P. S., “The Fluorescence Behavior and Stability of AgNP Synthesized by *Juglan Regia* Green Husk Aqueous Extract”. *Int. J. Nanosci. Nanotechnol.*, 15 (2019) 117-126.
  39. Nzekekwa, A. K., Abosede, O. O., “Green synthesis and characterization of silver nanoparticles using leaves extracts of neem (*Azadirachta indica*) and bitter leaf (*Vernonia amygdalina*)”, *Journal of Applied Sciences and Environmental Management*, 23(4) (2019) 695–699.
  40. Ghotekar, S., Pansambal, S., Pawar, S. P., Pagar, T., Oza, R., Bangale, S., “Biological activities of biogenically synthesized fluorescent silver nanoparticles using *Acanthospermum hispidum* leaves extract”, *SN Applied Sciences*, 1(11) (2019) 1342.
  41. Qayyum, S., Oves, M., Khan, A. U., “Obliteration of bacterial growth and biofilm through ROS generation by facilely synthesized green silver nanoparticles”, *PLOS ONE*, 12(8) (2017) e0181363.
  42. Fatema S., Shirsat M., Farooqui M., Arif P. M., “Biosynthesis of silver nanoparticle using aqueous extract of *Saraca asoca* leaves, its characterization and antimicrobial activity”, *Int. J. Nano Dimens*, 10 (2019) 163-168.
  43. Azarbani, F., Shiravand, S., “Green synthesis of silver nanoparticles by *Ferulago macrocarpa* flowers extract and their antibacterial, antifungal and toxic effects”, *Green Chemistry Letters and Reviews*, 13(1) (2020) 41–49.

44. Vala, A. K., Shah, S., "Rapid synthesis of silver nanoparticles by a marine-derived fungus *Aspergillus Niger* and their antimicrobial potentials", *Int. J. Nanosci. Nanotechnol*, 8 (2012) 197-206.
45. Jha, A. K., Prasad, K., Kulkarni, A. R., "Yeast mediated synthesis of silver nanoparticles", *Int. J. Nanosci. Nanotechnol*, 4 (2008) 17-22.
46. Chandrasekhara Rao, T., Lakshminarayana, G., Prasad, N. B. L., Sagan Mohan Rao, S., Azeemoddin, G., Atchynta Ramayya, D., Thirumala Rao, S. D., "Characteristics and compositions of *Carissa spinarum*, *Leucaena leucocephala* and *Physalis minima* seeds and oils", *J. Am. Oil. Chem. Soc.*, 61(9) (1984) 1472-1473.
47. Gamal-Eldeen, A.M., Amer, H., Helmy, W. A., Ragab, H. M., Talaat, R. M., "Antiproliferative and cancer-chemopreventive properties of sulfated glycosylated extract derived from *Leucaena leucocephala*", *Indian J. Pharm. Sci.*, 69(6) (2007) 805-811.
48. Deodhar, U. P., Paradkar, A. R., Purohit, A. P., "Preliminary evaluation of *Leucaena leucocephala* seed gum as a tablet binder", *Drug. Dev. Ind. Pharm.*, 24(6) (1998) 577-582.
49. Verma, P. R. P., Balkishen, R., "Studies on disintegrant action of *Leucaena leucocephala* seed gum in ibuprofen tablet and its mechanism", *J. Sci. Ind. Res.*, 66, (2007) 550-557.
50. Irene, M. V., Robert, M. T. G., Rosette, C. G., "Bioactivity studies on the alkaloid extracts from seeds of *Leucaena leucocephala*", *Phytother. Res.*, 11(8) (1997) 615-617.
51. Ademola, I. O., Akanbi, A. I., Idowu, S. O., "Anthelmintic activity of *Leucaena leucocephala* chromatographic seed fractions on gastrointestinal sheep nematodes", *Pharm. Biol.*, 45(7) (2005) 599-604.
52. Shrivastava, V. S., "Removal of Congo red dye from aqueous solution by *Leucaena leucocephala* (Subabul) seed pods" *International Journal of Chem Tech Research*, 4(3) (2012) 1038-1043.
53. Gutteridge, R. C., Shelton, H. M., "Forage Tree Legumes in Tropical Agriculture" *Tropical Grassland Society of Australia*, Australia (1998).
54. Selvaraj, R., Ramesh, V., Varadavenkatesan, T., "Green biosynthesis of silver nanoparticles using *Calliandra haematocephala* leaf extract, their antibacterial activity and hydrogen peroxide sensing capability" *Arabian. J. Chem.*, 10(2) (2015) 253-261.
55. Rakholiya, K., Chanda, S., "In vitro interaction of certain antimicrobial agents in combination with plant extracts against some pathogenic bacterial strains", *Asian Pac. J. Trop. Biomed.*, 2 (2012) 876-880.
56. Venkatesham, M., Ayodhya, D., Madhusudhan, A., Santoshumari, A., Veerabhadram, G., Girija Mangatayaru, K., "A Novel Green Synthesis of Silver Nanoparticles Using Gum Karaya: Characterization, Antimicrobial and Catalytic Activity Studies", *J. Clust. Sci.*, 25(2) (2014) 409-422.
57. Jegadeeswaran, P., Rajiv, P., Rajeshwari Shivaraj, P., Venkatesh, R., "Photo catalytic degradation of dye using brown seaweed mediated silver nanoparticles", *J. Bio. sci.*, 3(4) (2012) 229-233.
58. Zhang, W., Qiao, X., Chen, J., "Synthesis and characterization of silver nanoparticles in AOT microemulsion system", *Chem. Phy.*, 330(3) (2006) 495-500.
59. Parashar, U. K., Saxenaa, P., Srivastava, A., "Bioinspired synthesis of silver nanoparticles", *Dig. J. Nanomater. Biostruct.*, 4(1) (2009) 159-166.
60. Govindaraju, K., Tamilselvan, S., Kiruthogs, V., Simgaravelu, G., "Biogenic silver nanoparicles by *Solanum torvum* and their promising antimicrobial activity", *J. Biopest.* 3 (2010) 394-399.
61. Raut, R. W., Kolekar, N. S., Lakkakula, J. R., Mendhulkar, V. D., Kashid, S. B., "Photosynthesis of silver nanoparticles using *Gliricidia sepium* (Jacq)", *Curr. Nanosci.*, 5 (2009) 117-122.
62. Ramchandra Nalwade, A., Swati Sudhir, S., Gajanan Laxman, B., Namdeo Bhagwan, A., Sambhaji Dagadu, S., Vaishali Vasant, G., "Rapid biosynthesis of silver nanoparticles using bottle gourd fruit extract and potential application as bactericide", *Research in Pharmacy*, 3(3) (2013) 22-28.
63. Nestor, A. R. V., Mendieta, V. S., Lopez, M. A. C., Espinosa, R. M. G., Lopez, M. A. C., Alatorre, J. A. A., "Solventless synthesis and optical properties of Au and Ag nanoparticles using *Camiellia sinensis* extract," *Mater. Lett.*, 62(17) (2008) 3103-3105.
64. Nagajyothi, P. C., Sreekanth, T. V. M., Lee, J., Lee, K. P., "Mycosynthesis: Antibacterial, antioxidant and antiproliferative activities of silver nanoparticles synthesized from *Inonotus obliquus* (Chaga mushroom) extract", *J. Photochem. Photobiol. B*, 130 (2014) 299-304.
65. Huang, L., Zhai, M., Peng, J., Xu, L., Li, J., Wei, G. J., "A fluorescence quenching method for determination of copper ions with CdTe quantum dots", *J. Colloid Interface Sci.*, 316 (2007) 398-404.
66. Mat Yusuf, S. N. A., Che Mood, C. N. A., Ahmad, N. H., Sandai, D., Lee, C. K., Lim, V., "Optimization of biogenic synthesis of silver nanoparticles from flavonoid-rich *Clinacanthus nutans* leaf and stem aqueous extracts", *Royal Society Open Science*, 7(7) (2020) 200065.
67. Ramya juliet, M., "Biogenic synthesis of copper nanoparticles using aquatic pteridophyte *Marsilea quadrifolia* Linn. Rhizome and its antibacterial activity", *Int J Nano Dimens*, 11 (2020) 337-345.
68. Ghotekar, S., Savale, A., Pansambal, S., "Phytofabrication of fluorescent silver nanoparticles from *Leucaena leucocephala* L. leaves and their biological activities", *Journal of Water and Environmental Nanotechnology*, 3(2) (2018) 95-105.

69. Songa, J. Y., Janga, H. K., Kim, B. S., “Biological synthesis of gold nanoparticles using *Magnolia kobus* and *Diopyros kaki* leaf extracts”, *Process Biochem*, 44 (2009) 1133–1138.
70. Eya’ane Meva, F., Segnou, M. L., Okalla Ebongue, C., Ntomba, A. A., Belle Ebanda Kedi, P., Deli, V., Etoh, M. A., Mpondo Mpondo, E., “Spectroscopic synthetic optimizations monitoring of silver nanoparticles formation from *Megaphrynium macrostachyum* leaf extract”, *Revista Brasileira de Farmacognosia*, 26(5) (2016) 640–646.
71. Awwad, A. K. L. M., Salem, N. M., Abdeen, A., “Green synthesis of silver nanoparticles using carob leaf extract and its antibacterial activity”, *Int. J. Ind. Chem*, 4 (2013) 29-34.
72. Awwad, A. M., Salem, N. M., Ibrahim, Q. M., Abdeen, A. O., “Phytochemical fabrication and characterization of silver/silver chloride nanoparticles using *Albizia julibrissin* flowers extract”, *Adv. Matter Lett*, 6 (2015) 726–730.
73. Peron, S., Hadi, F., Azarbani, F., Ananda Murthy, H. C., “Antimicrobial, antioxidant, anti-glycation and toxicity studies on silver nanoparticles synthesized using *Rosa damascena* flower extract”, *Green Chemistry Letters and Reviews*, 14(3) (2021) 519–533.
74. Kaviya, S., Santhanalakshmi, J., Viswanathan, B., Muthumary, J., Srinivasan, K., “Biosynthesis of silver nanoparticles using citrus sinensis peel extract and its antibacterial activity”, *Spectrochim. Acta. A. Mol. Biomol. Spectrosc*, 79 (2011) 594–598.
75. Raut, R. W., Kolekar, N. S., Lakkakula, J. R., Mendhulkar, V. D., Kashid, S. B., “Extracellular synthesis of silver nanoparticles using dried leaves of *Pongamia pinnata* (L) pierre”, *Nano-Micro Letters*, 2(2) (2010) 106–113.
76. Muthuvel, A., Jothibas, M., Manoharan, C., “Synthesis of copper oxide nanoparticles by chemical and biogenic methods: Photocatalytic degradation and in vitro antioxidant activity”, *Nanotechnology for Environmental Engineering*, 5(2) (2020) 14.
77. Abebe, B., Zereffa, E. A., Tadesse, A., Murthy, H. C. A., “A review on enhancing the antibacterial activity of ZNO: Mechanisms and microscopic investigation”, *Nanoscale Research Letters*, 15(1) (2020) 190.
78. Biswal, A. K., Misra, P. K., “Biosynthesis and characterization of silver nanoparticles for prospective application in food packaging and biomedical fields”, *Materials Chemistry and Physics*, 250 (2020) 123014.
79. Yawadio Nsimba, R., Kikuzaki, H., Konishi, Y., “Antioxidant activity of various extracts and fractions of *Chenopodium quinoa* and *Amaranthus spp.* Seeds”, *Food Chemistry*, 106(2) (2008) 760–766.
80. Rajesh, R., Kumar, S. S., Venkatesan, R., “Efficient degradation of azo dyes using Ag and Au nanoparticles stabilized on graphene oxide functionalized with PAMAM dendrimers”, *New J. Chem*, 38 (2014) 1551–1558.